JPEDAV (2004) 25:528-537
DOI: 10.1361/15477020421052
1547-7037/$19.00 ©ASM International

Solid-Liquid Phase Equilibria in the Al-Fe-Si System at 727 °C

S. Pontevichi, F. Bosselet, F. Barbeau, M. Peronnet, and J.C. Viala

(Submitted April 13, 2004; in revised form September 02, 2004)

Different experimental techniques were combined to acquire better insight into the solid-liquid phase equilibria that tend to be established in the Al-Fe-Si ternary system at 727 °C under a pressure of 1 atm (101,350 Pa). Isothermal diffusion experiments followed by oil quenching were first carried out. The crystal nature, lattice parameters, morphology, and chemical composition of the different solid phases in equilibrium with the liquid were determined by x-ray diffraction, optical microscopy, scanning electron microscopy, and electron probe microanalysis. Points on the liquidus boundary were then positioned both directly by chemical analysis of liquid samples taken from solid-liquid mixtures equilibrated at 727 °C and indirectly by thermal analysis of Al-Si mixtures with controlled iron additions. On the one hand, it has been confirmed in agreement with currently accepted data that the compounds $\theta Al_{13}Fe_4$, $\alpha Al_{7.4}Fe_2Si$ (τ_5), and δAl_3FeSi_2 (τ_4) are in equilibrium at 727 °C with Al-Fe-Si liquids, the compositions of which have been refined. On the other hand, the authors have shown that the ternary compound γAl_3FeSi is in equilibrium at 727 °C with a ternary Al-Fe-Si liquid containing 10.5 to 16.5 at.% Si and 3.2 to 3.5 at.% Fe.

1. Introduction

Determination of the phase equilibria in the Al-Fe-Si ternary system is a key element in the development of materials based on aluminum alloys, notably with regard to the making of low-weight, high-strength aluminum-base castings for transport vehicles. Indeed, iron is one of the main impurities of aluminum, and silicon is the major addition element of most casting alloys. Furthermore, these two elements precipitate from the liquid alloys upon solidification to form hard and brittle Al-Fe-Si intermetallic compounds (Ref 1-8). Thorough knowledge of the phase equilibria in the Al-Fe-Si system, and more specifically of the solid-liquid equilibria, is thus essential to understand the solidification processes, to control the microstructure of the castings, and, eventually, to improve their mechanical performances.

With more than 15 reported stable binary or ternary compounds, the Al-Fe-Si system seems rather complex. Experimental data on these compounds and their relations in the Al-Fe-Si phase diagram have been summarized in well-documented review papers (Ref 2) and books (Ref 1, 9, 10). Recently, the enthalpies of formation of some of these compounds were measured (Ref 11-13). Attempts were also made to evaluate the Al-Fe-Si phase diagram by thermodynamic calculations (Ref 14-17). Considering the complexity of the system, it is not surprising on the one hand that some parts of the Al-Fe-Si phase diagram still need to be clarified. On the other hand, given the number of detailed studies carried out for more than 50 years on the aluminum-rich corner (the most relevant to casting), there should be no special reason to question the exactness of data reported in this corner.

During the course of an investigation on the reactivity between solid iron-base substrates and liquid Al-Si alloys, it appeared, however, that some reaction layer sequences experimentally observed could not be easily explained from the above cited literature data. This led the authors to reconsider the phase equilibria in the Al-Fe-Si ternary system. In the present work, particular attention is paid to the liquid-solid phase equilibria that tend to be established in the Al-rich corner of this system under a pressure of 1 atm (101,350 Pa) and at a temperature of 727 °C (1000 K). That value of 727 °C has been chosen since it corresponds to the highest temperature at which aluminum-base castings are generally processed. The stable solid phases likely to be in equilibrium with an aluminum-base liquid at that temperature have been listed in Table 1 with some of their specific features.

2. Experimental

Different techniques were used to acquire a better insight into the Al-Fe-Si solid-liquid phase equilibria. Isothermal heating treatments at 727 °C followed by oil quenching were first carried out to determine the crystal nature and composition of the solid phases coexisting with the liquid. Complementary experiments were then undertaken to determine the position of the solid-liquid boundary both indirectly by thermal analysis of Al-Si mixtures with controlled iron additions and directly by chemical analysis of the liquid in solid-liquid mixtures equilibrated at 727 °C.

2.1 Isothermal Heating Followed by Oil Quenching

Mixtures of commercial powders of aluminum (purity > 98 wt.% with oxygen as main contaminant, grain size $d <$ 160 μm, Fluka, Buchs, Switzerland), iron (purity > 99.5

S. Pontevichi, F. Bosselet, F. Barbeau, M. Peronnet, and **J.C. Viala,** Laboratoire des Multimatériaux et Interfaces, UMR CNRS n° 5615, Université Claude Bernard Lyon 1, F-69622 Villeurbanne Cedex, France. Contact e-mail: viala@univ-lyon1.fr.

Table 1 Stable compounds reported in the Al-rich corner of the Al-Fe-Si ternary system

Chemical compound	Chemical formulae Density, *d*	Homogeneity range near 727 °C, at.% (wt.% in parentheses)	Symmetry, structure, cell parameters, nm, diffraction data used for characterization	Decomposition temperature, °C
θ	Al_3Fe $Al_{13}Fe_4$ *d* = 3.90	From Ref 3, 18-20 Fe: 23.5-25 (38.6-41.1) Si: 0-5 (0-4.5)	Monoclinic, *C2/m* *a* = 1.5492(2), *b* = 0.8078(2), *c* = 1.2471(1), β = 107.69(1)° (Ref 19, 21) XRD spectrum recalculated from Ref 21	1152 (Ref 18, 22)
α = τ_5 also referred to as α_H in Ref 24 and α′ in Ref 4	$Al_{12}Fe_3Si_2$ Al_8Fe_2Si $Al_{7.4}Fe_2Si$ *d* = 3.58	From Ref 3, 23, 24 near 600 °C Fe: 18.5-21.5 (32-36) Si: 7-13 (6-11) Refined (Ref 20, this work) Fe: 18-19.5 (31-33.3) Si: 10-12.5 (8.6-10.9)	Hexagonal, $P6_3/mmc$ (Ref 23, 25) *a* = 1.2404(1), *c* = 2.6234(2) with 44.9Fe, 167.8Al, and 23.9Si atoms per unit cell (Ref 26) JCPDS 41-894 and 71-238	855 (Ref 9) 715 (Ref 16) 710 (Ref 1)
β = τ_6	Al_5FeSi $Al_{4.5}FeSi$ $Al_9Fe_2Si_2$ *d* = 3.3 to 3.35	From Ref 3, 20, 24, 27 at 640 °C Fe: 15.5-16.5 (27-29) Si: 17-19 (15-17)	Monoclinic, *A2/a* *a* = 0.6161(3), *b* = 0.6175(3) *c* = 2.0813(6); β = 90.42(3)°, (Ref 8, 28) XRD spectrum re-calculated from Ref 28	700 (Ref 1) 694 (Ref 16) 667 ± 5 (Ref 20)
γ termed τ2 in Ref 9 and τ7 in Ref 16, 17	Al_3FeSi $Al_5Fe_2Si_2$ *d* = 3.75	From Ref 3, 25 Fe: 18-23 (31-38) Si: 12.5-22 (11-18.5) Refined (Ref 20, this work) Fe: 19.5-21.5 (33-36) Si: 15.2-25.6 (13-22)	Monoclinic *a* = 1.78, *b* = 1.025, *c* = 0.890, β = 132° (Ref 25) no structure determination JCPDS 20-0032	940 (Ref 9) 850 (Ref 16)
δ = τ_4	Al_4FeSi_2 Al_3FeSi_2 $Al_{2.7}FeSi_{2.3}$ *d* = 3.3 to 3.4	From Ref 29 Fe: 15-17 (26.5-29.5) Si: 27-43 (24-38) Refined (Ref 20, this work) Fe: 15.5-16.5 (27-29) Si: 30.5-38 (27-33)	Orthorhombic, *Pbcn* *a* = 0.6061, *b* = 0.6061, *c* = 0.9525 (Ref 29) XRD spectrum recalculated from Ref 29	865 (Ref 9) 834 (Ref 16)
τ2 in Ref 2, τ3 in Ref 9, τ23 in Ref 16, 17	Al_2FeSi	From Ref 30, 17 Fe: 25 (40.5) Si: 25 (20.4)	Orthorhombic, *Cmma* *a* = 0.7995, *b* = 1.5162; *c* = 1.5221 (Ref 30) XRD spectrum calculated from Ref 30	935 (Ref 2, 9) 920 (Ref 16)
τ″ (Ref 17)	$Al_4Fe_{1.7}Si$	From Ref 31, 17 Fe: 25.4 (41.2) Si: 14.9 (12.1)	Hexagonal, $P6_3/mmc$ *a* = 0.7509, *c* = 0.7594 (Ref 31) XRD spectrum calculated from Ref 31	?

Note: Data are from Mondolfo (Ref 1), Rivlin and Raynor (Ref 2), Ghosh (Ref 9), Liu and Chang (Ref 16), Raghavan (Ref 17), and more specific references given in the table (other compounds with a smaller aluminum content also exist).

wt.%, grain size $d < 150$ μm, Merck, Darmstadt, Germany), and silicon (purity > 99 wt.%, grain size $d < 100$ μm, Merck) were ball-homogenized and cold-pressed under 200 MPa into small pellets (13 mm in diameter and 4 mm in height). Each pellet was then placed in a graphite crucible and heated at 727 °C under purified argon, using the experimental setup shown in Fig. 1. At the end of the isothermal treatment, the crucible with its pellet inside was dropped in paraffin oil at ~5 °C.

2.2 Thermal Analysis of Al-Si Mixtures with Controlled Iron Additions

Binary Al-Si alloys with known silicon contents were first prepared from commercial ingots of aluminum (A5LR Pechiney, Alcan, France, Al > 99.5 wt.%, Fe: 0.23 wt.%, Si: 0.07 wt.%, other elements Mg, Ti, V, Cr, Mn, Ni, Cu, Zn < 0.01 wt.%), Al-Si alloy (A-S13 Pechiney, Si: 12.6 wt.%, Fe: 0.42 wt.%, same other elements as in A5LR < 0.01 wt.%) and from 6N pure single-crystalline silicon wafers. For each experiment, a mass of 60 g of these constituents was melted by radio frequency (rf) heating in an oxide crucible lined with αAl_2O_3 powder. Temperature was measured with a precision better than ±0.2 °C by plunging in the melt a K-type (Ni/Cr) thermoelectric couple. Known quantities of iron were dissolved step-by-step in the melt by immersing in it small rods (6 × 6 × 30 mm) of cold-pressed powders containing 20 at.% Fe and having the same Al:Si atomic ratio than the binary alloy melt. Four to six successive iron additions were made up to an iron content of about 4 at.%.

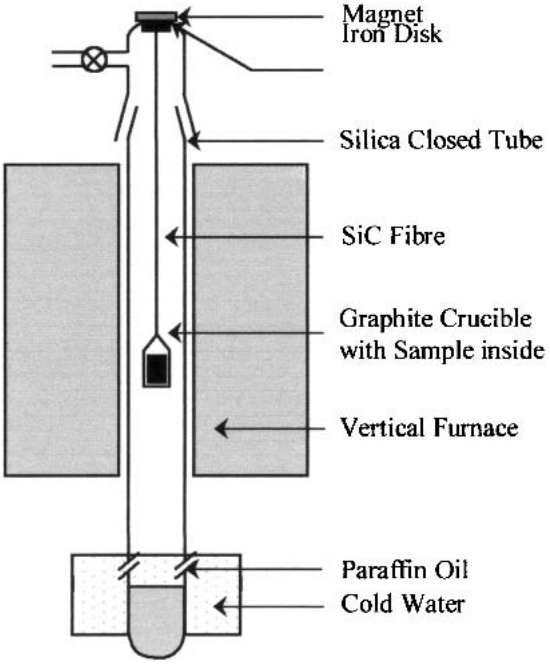

Fig. 1 Experimental setup used for isothermal heating and subsequent oil quenching

The quantity of iron initially contained as impurity in the binary alloy melt was taken into account to determine the exact iron content in the melt.

Direct thermal analysis curves were obtained by recording the Al-Fe-Si alloy temperature versus time upon cooling at different rates ranging from 50 to 5 °C/min. The first change in the slope of the cooling curve yielded a temperature, T_c, corresponding to the exothermic nucleation and growth from the liquid of solid crystals. A pure aluminum standard used for calibration gave a crystallization temperature of 660.6 °C, whatever the cooling rate. Differential thermal analysis (DTA; Setaram TG-DTA 92-12, Caluire, France) was also used to determine the temperature of crystallization of some Al-Fe-Si liquids upon cooling. In that case, the samples were small ingots weighing about 50 mg that were sawed in rods sucked from 60 g melts, and the cooling rates varied from 10 to 1 °C/min. It is to be noted that due to thermal phenomena that were too diffuse (above the eutectic temperature), the DTA curves could not be exploited on heating.

2.3 Taking of Liquid Samples

Samples of liquid were taken from alloy melts by sucking through a silica tube (inner and outer diameters: 4 and 6 mm, respectively). To avoid metal/oxide reaction, the silica tube was previously lined with carbon black. Solidification of the melt in the carbon-lined silica tube upon sucking was almost instantaneous, and fine-grained homogeneous rods 10 to 30 mm in length were obtained.

2.4 Solid Sample Characterization

Solid samples were characterized by x-ray diffraction (XRD), optical metallography (OM), scanning electron microscopy (SEM), electron probe microanalysis (EPMA), and chemical analysis (CA). The XRD spectra were recorded on grossly polished sections, using standard diffraction equipment (Philips PW1817 diffractometer, Cu Kα radiation) (Panalytical, Eindhoven, The Netherlands). To avoid erroneous indexing, a pure powder sample of the first five compounds reported in Table 1 was synthesized and an XRD spectrum was recorded. For two compounds (α and γ, Table 1), the diffraction lines of the synthesized samples matched well the JCPDS data (International Center for Diffraction Data, Newton Square, PA). For the other three (θ, δ, and β) a better match was found when angular positions and intensities recalculated from published single crystal structure data were used as reference (Table 1). OM and SEM observations were made on diamond polished sections. EMPA were carried out using a Camebax apparatus (Cameca, Courbevoic, France) operated under an accelerating voltage of 10 kV. After background subtraction, the counting rates obtained for Al, Fe, and Si were referred to those recorded under the same conditions on pure and freshly polished standards. After correction for atomic number, absorption, and fluorescence, metal contents in atomic percent were obtained within an absolute error bar not higher than ±1 at.% for Al and Si. Chemical analyses were also performed at Analysis Central Service, National Center for Scientific Research (SCA CNRS), (Vernaison, France) by plasma emission spectroscopy after chemical dissolution to determine the mean composition of solid samples taken from aluminum-base melts.

3. Results

3.1 Isothermal Diffusion Experiments

In this first set of experiments, powder mixtures of aluminum, iron, and silicon were isothermally heated at 727 ± 3 °C for 72 h and oil quenched. The iron content of these mixtures was initially fixed at 15 wt.% (7.87 to 7.99 at.%) so that the volume fraction of the liquid in the treated samples remained higher than 50%, ensuring fast reaction-diffusion. As to the silicon content, it was varied from 3 to 42 at.% to cross all the possible liquidus surfaces. The initial composition of each of the mixtures that were prepared is given in Table 2. During isothermal heating at 727 °C, chemical reactions developed in these mixtures and equilibrium conditions tended to be established between one or two solid compounds and the liquid phase. From the results of preliminary experiments, it took about 45 h for reaction completion at that temperature. To ensure complete equilibration, the heating time of each pellet was increased to 72 h. At the end of that period of time, the two- or three-phased equilibria thus established were "frozen" by oil quenching. Such a violent quenching procedure was necessary to avoid or limit the development of fast liquid-solid transformations upon cooling. The crystal nature and chemical composition of solid compounds formed in the as-treated mixtures were characterized by XRD and EPMA; the results are summarized in Table 2. Concerning EPMA, each composition reported in the table is the average of at least ten determina-

tions on different crystals of the same phase in a given sample.

For mixtures with a silicon content of 3 and 5 at.%, θ was the major solid phase characterized by XRD after reaction at 727 °C. Observed by OM and SEM, the θ phase appeared under the form of platelets (up to 150 μm in lateral extension and 20 μm in thickness) embedded in a fine-grained Al-rich metal matrix. The size of the Al grains was in the range 10 to 15 μm, from which a cooling rate of the order of 100 °C/s was estimated when crystallization started. A great number of small liquid inclusions were observable within the θ platelets. The presence of these inclusions rendered difficult a precise analysis of θ by EPMA and chemical compositions reported in Table 2 for that phase may be slightly shifted toward lower iron contents. This small shift did not notably affect the silicon contents measured by EPMA, and, in agreement with previous reports (Ref 9), it was confirmed that a few percent of silicon atoms were incorporated in the framework of θ. The variation in θ cell parameters resulting from that incorporation remained within the limits given in Stefaniay et al. (Ref 3).

To continue with the silicon-poor mixtures (samples 3, 5, and 6), a set of weak XRD lines remained unindexed on the basis of data reported in Table 1 (in addition to the lines characteristic for θ, Al, and Si). Referring to literature data on metastable Al-Fe-Si phases, most of these lines could be indexed in the cubic unit cell of the metastable phase α_C-AlFeSi with $a = 1.25$ nm described in Turmezey et al. (Ref 8, 24) and previously referred to as μ_1 by Ghosh (Ref 9). The α_C metastable phase formed a thin layer (1 to 2 μm thick) at the surface of θ platelets. Due to its small thickness, chemical analysis of this layer by EPMA was difficult. An approximate composition Al:Fe:Si = 74:16:10 at.% could, however, be found in sample 5, where α_C was the most abundant (relatively). That composition is in good agreement with the data reported for μ_1 or α_C (Ref 8, 9). The α_C-AlFeSi metastable phase is known to crystallize from Al-Fe-Si alloys upon rapid cooling (Ref 24). It can then be concluded that the metastable α_C phase present in the authors' samples has formed upon quenching.

From these first results, it appears that the cooling rate is fast enough to avoid detectable reaction and transformation upon cooling of the solid phases in equilibrium at 727 °C with the liquid. In that sense, the phase equilibria established at 727 °C can be considered as frozen by oil quenching. However, crystallization upon cooling of ternary com-

Table 2 Crystal nature (XRD) and chemical composition (EPMA) of the solid compounds formed in Al-Fe-Si powder mixtures equilibrated at 727 °C and oil quenched

	Initial composition, at.%			Solid compounds characterized	Composition as determined by EPMA, at.%		
Sample	Al	Si	Fe	by XRD	Al	Si	Fe
3	89	3.13	7.87	θ(a)	74.4	2.0	23.6
5	86.9	5.22	7.87	θ(a)	74.3	2.6	23.1
6	86.03	6.09	7.88	θ(a) (b)	73.4	3.9	22.7
6b	85.86	6.26	7.88	θ	73.6	3.0	23.4
				α	70.6	10.3	19.1
7	84.81	7.31	7.88	θ	75.4	2.9	21.8
				α	71.8	10.7	17.5
8	83.76	8.36	7.88	α	70.9	10.3	18.8
9	82.71	9.41	7.89	α	70.3	11.9	17.8
10	81.41	10.7	7.89	α	68.5	12.0	19.5
11	80.6	11.51	7.89	α	69.1	13.1	17.8
				γ	64.2	16.4	19.4
12	79.19	12.91	7.90	γ	62.6	16.3	21.1
13	78.49	13.61	7.90	γ	62.8	17.2	20.0
15	76.37	15.72	7.91	γ	60.9	18.7	20.4
16	75.29	16.80	7.91	γ	60.9	19.3	19.8
17	74.25	17.83	7.91	γ	59.6	19.9	20.5
				δ	53.8	30.5	15.7
19	72.13	19.95	7.92	γ	60.2	20.3	19.5
				δ	52.8	31.0	16.2
22	70.0	22.07	7.93	δ	52.5	31.2	16.3
25	67.06	25	7.94	δ	52.8	31.4	15.8
42	49.63	42.38	7.99	δ	49.1	34.4	16.5

(a) Weak XRD lines attributable to the metastable α_c phase (with Al:Si:Fe ≈ 74:10:16 at.%) were also observed. (b) Two α crystals were found by OM in another section of this sample.

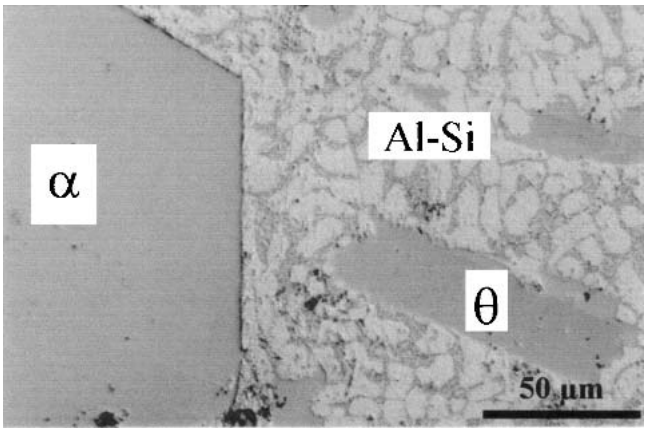

Fig. 2 Typical morphology of the θ and α phases coexisting at 727 °C in sample 7 (optical microscopy)

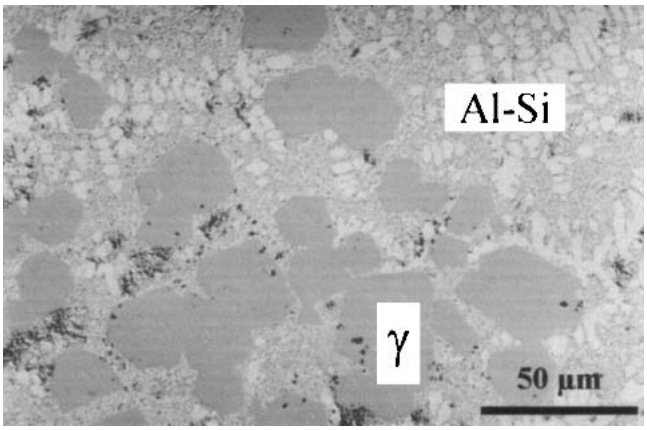

Fig. 3 Typical morphology of the γ phase formed at 727 °C in sample 13 (optical microscopy)

pounds from the liquid oversaturated in iron cannot be avoided. This concerns α_c that crystallizes on θ and also β that can form small platelets in the liquid from 667 °C down to 576 °C, the temperature of the Al-Si-β-L ternary eutectic.

In samples 6b and 7, which contained 6.26 and 7.31 at.%Si, respectively, a second intermetallic phase was unambiguously characterized by XRD with θ. That new phase was the ternary intermetallic compound α under its stable hexagonal variety (also referred to as α_H or τ5, Table 1). The diffraction lines attributable to metastable α_C were no longer detected, although a discontinuous layer of that phase was still observable by OM at the surface of a few θ platelets. Examined by OM and SEM, α appeared under the form of big globular crystals up to 200 μm in diameter with faces exhibiting hexagonal shapes, as illustrated in Fig. 2. Some liquid pools were present near the center of the α crystals but these were less numerous than in θ. Analyses by EPMA performed in different points of an α crystal (inner and outer part) as well as on different α crystals gave the same results, indicating a good homogeneity, and these results were within the composition range previously reported for the α-phase (Table 1). As to sample 6 with 6.09 at.% Si, it also contained in addition to θ two big crystals of the α type observable by OM, but these did not appear in the section examined by XRD.

For samples 8, 9, and 10, neither θ nor the α_C metastable phase were detected by XRD. In fact, α was the only intermetallic phase characterized by XRD and observable by OM and SEM. The morphology of the α crystals (big globular crystals with hexagonal shapes) remained the same while their silicon content increased from 10.3 to 12 at.%. An increase of the silicon content has been reported to cause a slight contraction (~2×10^{-3}) of the hexagonal unit cell of α (Ref 24). In the present experiments, the change in the cell parameters of α between samples 8 and 10 was not significant.

As the silicon content in the initial mixtures became higher than 11 at.%, the diffraction lines of another solid phase appeared in the XRD spectra. That phase was unambiguously characterized as the γ ternary compound reported in Table 1. First coexisting with α in sample 11, γ was the only intermetallic compound detected in samples 12, 13, 15, and 16. As shown in Fig. 3, the γ ternary compound appeared under the form of globular faceted crystals with small liquid inclusions, like α previously. However, the size of the crystals was much smaller: 15 to 30 μm for γ instead of 100 to 200 μm for α. As revealed by EPMA, the silicon content in γ increased from 16.4 to nearly 20 at.%, whereas the iron content remained approximately constant. Aluminum and iron atoms may then exchange their positions in the crystal structure of γ. In correlation, the angular positions of most of the XRD lines characteristic for γ, that matched very well the JCPDS data file 20-0032 (International Center for Diffraction Data, Newton Square, PA) in samples 12 and 13, were gradually shifted toward larger angles in samples 15 and 16. This means that the unit cell volume of γ decreases when the Si/Al ratio increases, which is consistent with the smaller atomic radius of Si atoms.

A fourth phase corresponding to the ternary compound δ was characterized by XRD after heat treatment of mixtures with initial silicon contents higher than 17 at.%. Mixed with γ in samples 17 and 19, compound δ was the only intermetallic phase characterized in the three samples the richest in silicon, namely samples 22, 25, and 42. As shown in Fig. 4, the ternary compound δ appeared under the form of 30 to 60 μm faceted crystals with rectangular shape. When the silicon content in the initial mixture increased, the silicon content of the δ crystals increased from 30.5 to 34.4 at.%, whereas their iron content remained constant. In Fig. 4, the δ crystals coexist with large blocks of elemental silicon. It can be remarked that when a silicon block is present, growth of δ has stopped. This indicates that solid silicon blocks

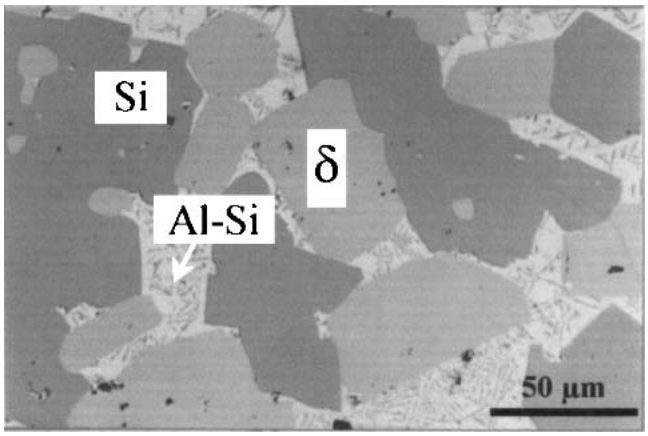

Fig. 4 Typical morphology of the δ phase coexisting at 727 °C with Si blocks in sample 42 (δ: light grey; Si: dark grey; optical microscopy)

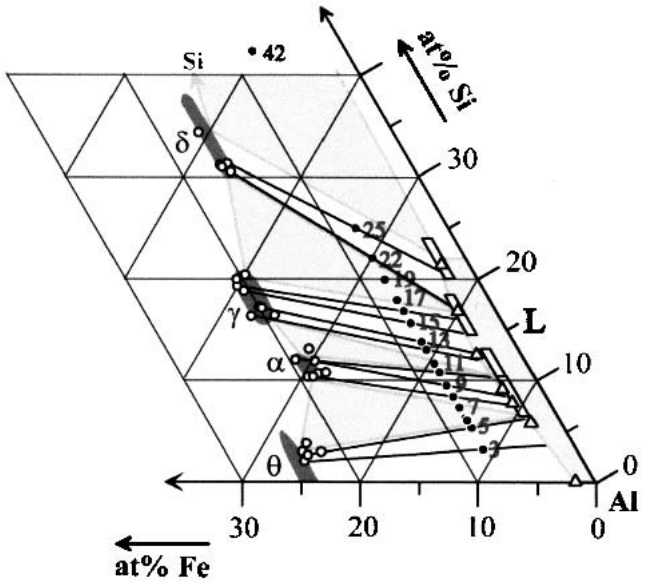

Fig. 5 Results obtained in the Al-Fe-Si system by isothermal heating (filled and open circles), chemical analysis of liquids taken from equilibrated samples (distorted rectangles), and thermal analysis (open triangles). Experimental tie lines have been drawn in two-phase fields (solid dark straight lines).

were present in sample 42 during isothermal heating at 727 °C.

Figure 5 summarizes the results of this first set of experiments in terms of phase equilibria in the Al-Fe-Si section at 727 °C. Tie lines passing by a point representative of a given mixture (filled circle) and the point representative of the compound produced by reacting that mixture (open circle) have been drawn in the two-phase fields. To obtain points on the liquidus line at the other end of these tie lines, it would theoretically have sufficed to determine the average composition of the metal matrix embedding the crystals in the treated samples. In fact, such a determination was not possible. Effectively, although fine-grained, the rapidly solidified Al-Fe-Si alloy surrounding the solid phases gave too much scattered results when analyzed by EPMA. This is the reason why determinations by chemical analysis and thermal analysis were undertaken.

3.2 Chemical Analyses

Chemical analyses were performed on liquids taken from S_1-S_2-L three-phase samples equilibrated at 727 °C. To

Table 3 Composition of liquids in S_1-S_2-L samples equilibrated at 727 °C directly determined by chemical analysis

Sample	Three-phase equilibrium reached at 727 °C	Composition of the liquid in equilibrium with S_1 and S_2 at 727 °C, at.%		
		Al	Si	Fe
CA1	θ-α-L	88.8	8.4 ± 2	2.8 ± 0.5
CA2	α-γ-L	85.9	11.2 ± 2	2.9 ± 0.5
CA3	γ-δ-L	80.5	16.3 ± 2	3.2 ± 0.5
CA4	δ-Si-L	75.6	22 ± 2	2.4 ± 0.5

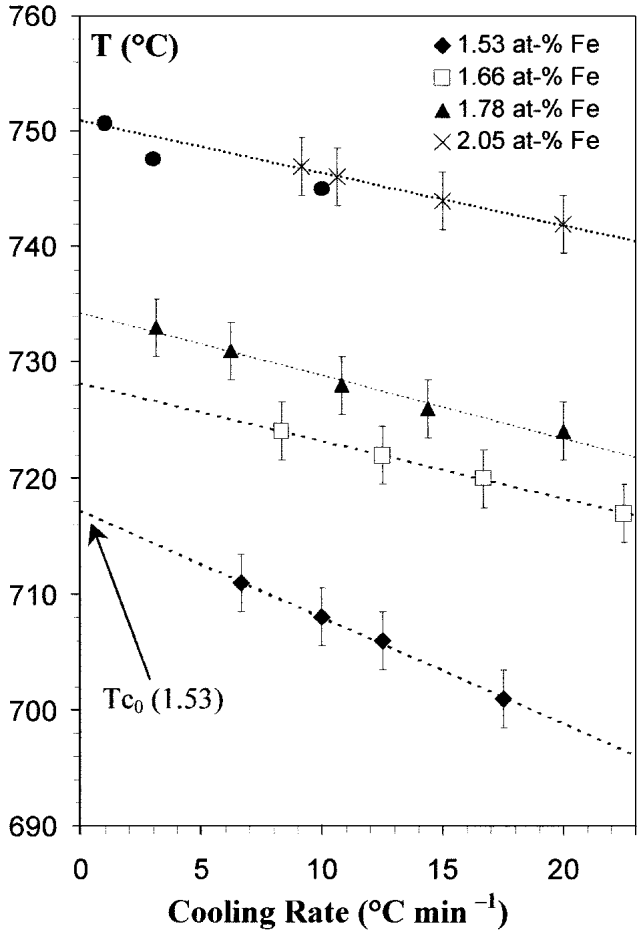

Fig. 6 Thermal analysis experiments: temperature of crystallization of θ from binary Al-Fe melts as a function of the cooling rate, for different iron contents in the liquid (filled circles show DTA results)

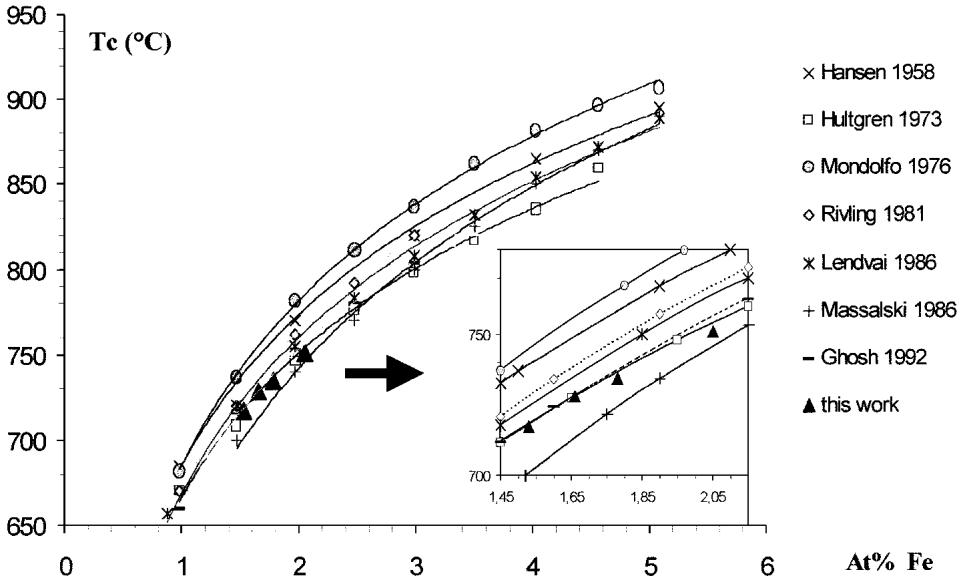

Fig. 7 The solubility of iron in liquid Al (Fe-Al liquidus line), according to different literature data sources and from the thermal analysis experiments carried out in this work

avoid solid crystals being carried along by the liquid upon sucking, a special procedure was used to prepare these samples. A rod (5 × 6 × 30 mm, weight 4 g) consisting of a body of two conjugate solids soaked in a solidified Al-Fe-Si alloy was first produced by heating for 150 h at 727 °C under argon a mixture of appropriate composition. For example, that composition was Al:Fe:Si = 75:18:7 at.% for a θ-α alloy rod. Once cooled to room temperature, the rod was broken into three to four pieces and immersed in an Al-Si melt separately prepared. That melt (10 g Al-Si alloy with 7 at.% Si for the given example) was contained in a small cylindrical alumina crucible (16 mm in inner diameter, 28 mm in height) where it was held at 800 °C by conventional radiation heating. Fifteen minutes after immersion, the temperature was slowly decreased to 727 °C and fixed at that value for 72 h. Equilibrium conditions could thus be established between the liquid alloy and the two solid phases without nucleation of solid crystals in the liquid. Indeed, equilibration essentially proceeded by mixing of liquids and partial dissolution of solids. Liquids taken from such samples were then free of floating crystals and had a composition representative of the equilibrium state.

Table 3 lists the compositions found by chemical analysis for different Al-Fe-Si liquids taken from specially prepared three-phase samples S_1-S_2-L. These compositions (distorted rectangles in Fig. 5) are consistent with the literature data on the Al-Fe-Si phase diagram and with the isothermal diffusion results reported in Fig. 5. However, the iron, and especially the silicon, contents are affected by large error bars attributable to the chemical analysis procedure (incomplete dissolution and overlapping problems). As attempts to reduce these error bars failed, such direct determinations were not continued.

3.3 Thermal Analysis Experiments

To obtain more detailed information on the liquidus line in the Al-Fe-Si section at 727 °C, indirect determinations were undertaken by thermal analysis (TA). These TA experiments were first carried out in the Al-Fe binary system for which literature data are available from different sources (Ref 1, 2, 9, 18, 22, 32, 33). It was thus possible to check the validity of the experimental procedure developed. Controlled iron additions were made to a pure aluminum melt and the temperatures of appearance of the first crystals of θ from the melt, T_c, were determined by TA upon cooling. By reheating some samples at 900 °C and repeating the T_c

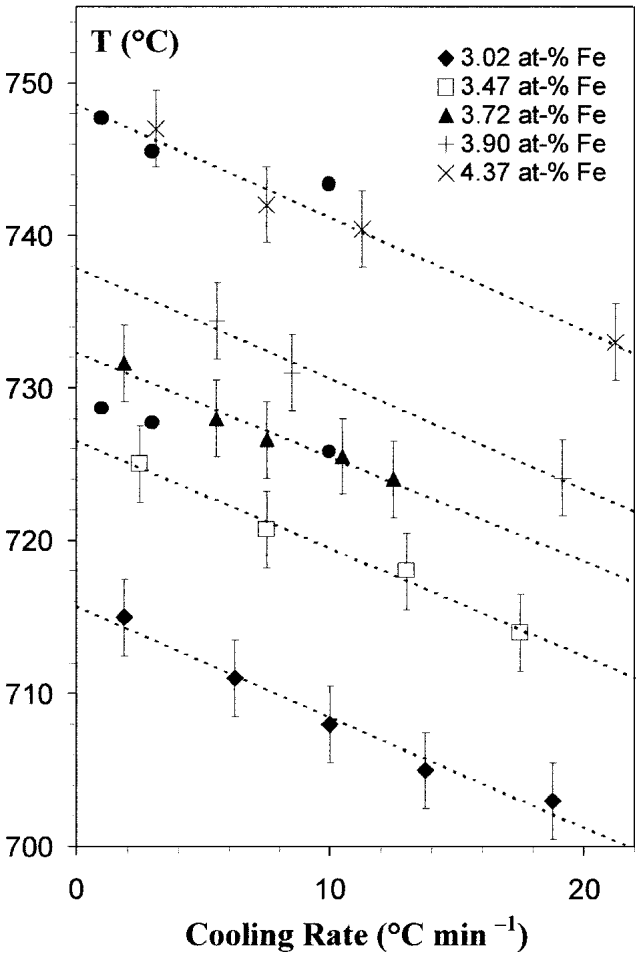

Fig. 8 Example of thermal analysis measurements: variation with the cooling rate of the temperature of crystallization of γ from a ternary Al-Fe-Si melt with a Si/Al + Si ratio fixed at 13 at.% and to which increasing amounts of iron have been added (filled circles show DTA results)

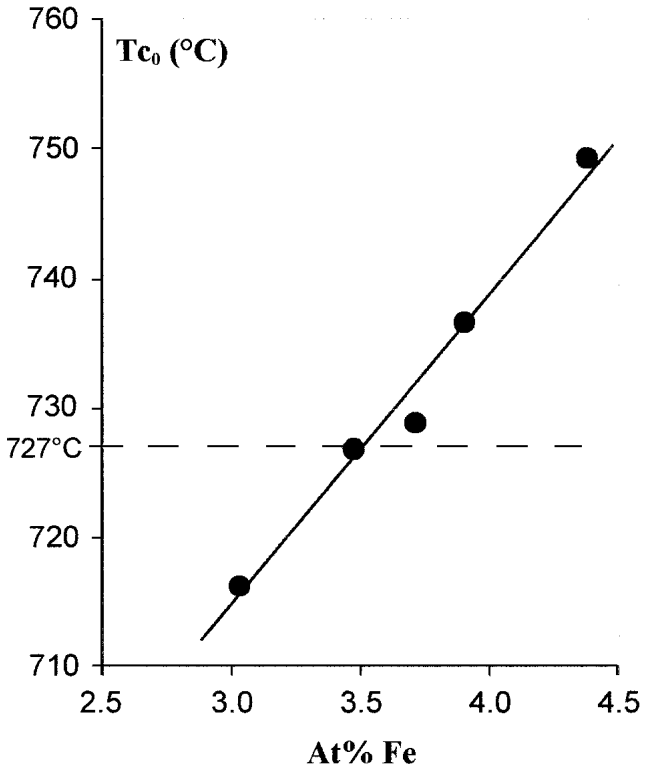

Fig. 9 Exploitation at null cooling of the thermal analysis results reported in Fig. 8: temperature of crystallization of γ from a melt with an atomic ratio Si/Al+Si of 13 at.% as a function of the iron content in the melt

determination upon cooling, very reproducible results were obtained on condition that the cooling rate did not change. In fact, whereas a constant temperature of 655 °C was found at any cooling rate for the eutectic transformation, T_c was observed to increase when the cooling rate decreased. Consequently, several cycles were systematically made after each iron addition at different cooling rates ranging from 50 to 5 °C/min (below 5 °C/min, the change in slope of the TA curve was very difficult to detect). In Fig. 6 the T_c values obtained after four successive iron additions are plotted as a function of the cooling rate. It can be seen that for each addition, T_c exhibits a nearly linear dependence with the cooling rate. A regression line was then drawn to attain the value of T_c at null cooling rate T_{c0}, i.e., under quasi-equilibrium conditions. To compare direct and differential thermal analysis, a sample of the melt with the highest percentage of iron added (2.05 at.%) was taken and analyzed by DTA at three different cooling rates, 10, 3, and 1 °C/min. From the results reported under the form of grey circles in Fig. 6, it can be verified that, within the error bar, the same T_c values with the same cooling rate dependence were obtained by both TA and DTA.

The four T_{c0} values extrapolated at null cooling rate from the results reported in Fig. 6 have been plotted as a function of iron added in Fig. 7. In that figure different liquidus lines reported in the literature concerning the L-θ equilibrium for the Al-Fe binary system near 730 °C have also been drawn. It can be seen that the crystallization temperatures, T_{c0}, determined by TA experiments (filled triangles) are in good agreement with the most recently reported L-θ liquidus lines in the Al-Fe binary phase diagram. By simple interpolation of the TA measurements reported in Fig. 6, a value of 1.66 ± 0.05 at.% Fe was found for the solubility of iron in liquid aluminum at 727 °C.

Thermal analysis experiments were then extended to Al-Fe-Si liquid alloys. As an example, Fig. 8 shows the T_c values determined upon cooling for alloys with a Si/Si + Al ratio of 13 at.%. Again, TA and DTA gave the same results and a linear dependence of T_c with the cooling rate was observed. Linear extrapolation at null cooling rate led to different T_{c0} values. As previously, these T_{c0} values were plotted as a function of the melt iron content to obtain points on the liquidus line of the Al-Fe-Si phase diagram in the Fe-Al87Si13 at.% isopleth (i.e., in the vertical section corresponding to a constant Si/Si + Al ratio of 13 at.%). From the results reported in Fig. 9, the solubility at 727 °C of iron in an Al-Si alloy with an initial silicon content of 13 at.% was found to be of 3.5 ± 0.1 at.% Fe.

By repeating the same procedure on alloys with initial silicon contents of 6, 8, 9, 17.5, and 22 at.%, different values of the solubility of iron in Al-Si melts at 727 °C were obtained. The values are reported in Table 4, and the corresponding points of the solid-liquid boundary in the 727 °C section of the Al-Fe-Si phase diagram have been plotted in Fig. 5 (open triangles). For each Si/Si + Al ratio, the crystal nature of the solid phase in equilibrium with the liquid near 727 °C was determined. This was achieved by immersing a small alumina rod at 740 °C in the melt the richest in iron and characterizing by XRD the crystals deposited at the surface of that rod upon cooling from 740 to 715 °C. The XRD results thus obtained (Table 4, right column) were in good agreement with the tie lines drawn in the two-phase fields in Fig. 5.

4. Discussion

Three complementary approaches have been used to investigate the solid-liquid phase equilibria at 727 °C in the Al-Fe-Si ternary system. Isothermal diffusion experiments have brought precious information on the crystal nature and composition of the solid phases involved in these equilibria. More specifically, the results of these experiments clearly show that among the aluminum-rich compounds listed in Table 1, only four of them are effectively in equilibrium with the aluminum-base liquid at 727 °C; these are θ, α, γ, and δ. The problem was a determination of the composition of the liquid at the end of tie lines or at the corner of tie triangles. This was achieved directly by chemical analysis of liquids taken from equilibrated samples and indirectly by thermal analysis of Al-Si alloys with controlled iron additions. As a matter of fact, much more precise results were obtained using the indirect method. At this point, the issue was to combine the present experimental results with literature data to provide an Al-Fe-Si section at 727 °C as precisely and self-consistently as possible.

It was first necessary to define the homogeneity range of each of the solid phases involved in solid-liquid equilibria. Concerning the iron content, it can be remarked that the

Table 4 Composition of different points of the liquidus line at 727 °C, indirectly determined by thermal analysis

Sample	Initial composition of the liquid before iron addition Si/Al + Si, at.%	Iron addition needed to saturate the liquid at 727 °C, at.%	Composition of the liquid in equilibrium with S at 727 °C Al:Si:Fe, at.%	S-L equilibrium between 740 and 720 °C, as verified by XRD
TA0	0	1.66 ± 0.05	98.34:0:1.66	θ-L
TA1	6	2.4 ± 0.15	91.74:5.86:2.4	θ-L
TA2	8	3.0 ± 0.1	89.24:7.76:3.0	α-L
TA3	9	3.2 ± 0.1	88.09:8.71:3.2	α-L
TA4	13	3.5 ± 0.1	83.95:12.55:3.5	γ-L
TA5	17.5	3.2 ± 0.1	79.86:16.94:3.2	γ-L
TA6	22	2.4 ± 0.1	76.13:21.47:2.4	δ-L

compositions reported in Table 2 for these solid phases all correspond to the side of their homogeneity range facing the liquid, i.e., the side poorest in iron. These compositions were compared with literature data (Table 1) and with the results of other analyses performed in a parallel study on the same phases but at the other side of the homogeneity range (the solid-state side richest in iron). The comparison led the authors to consider that the homogeneity ranges relative to iron for the four stable compounds encountered in the present work were narrow (from 18 to 19.5 at.% Fe for α, from 23.5 to 25 at.% Fe for θ, and from 19.5 to 21.5 at.% Fe for γ) or very narrow (no larger than ±1 at.% Fe for δ). On the other hand, these compounds are known to possess a noticeable range of existence with regard to their silicon content (Table 1). To evaluate the extent of this silicon homogeneity range at 727 °C, the analytical results of the present work were combined with other analyses performed on samples equilibrated in the solid state and with literature data. This led to the representation given in Fig. 10. It should be remarked that all the possible silicon compositions on the iron-poor limit of each range represented are not necessarily in equilibrium with a liquid; some of these compositions are in equilibrium with solids only. Another remark is concerned more specifically with the range of existence relative to the silicon content of the compound α. At a temperature of about 600 °C, a range of 8.2 to 11.1 at.% Si (7 to 9.5 wt.% Si) is reported for that compound by Griger (Ref 23), whereas the authors' results give a range of 10 to 12.5 at.% Si (8.6 to 10.9 wt.% Si). This outward discrepancy would in fact mean that the range of existence of α is not only narrowed but also shifted toward higher Si contents when the temperature increases above 600 °C.

A second goal was to locate in Fig. 10 the position of the corners of the different three-phase triangles S_1-S_2-L. For each corner located on the solidus of a compound, the silicon content was logically defined as the average of the contents measured for this compound by EPMA in the relevant three-phase samples listed in Table 2. As to the four corners located on the liquidus line, their position was more difficult to determine. On the one hand, that position directly followed from the results reported in Table 3, but these were imprecise. On the other hand, precise and accurate points on the liquidus line were obtained by thermal analysis (coordinates in Table 4), but these points corresponded only to the end of tie lines in two-phase fields. Referring to general principles applicable to phase diagrams (Ref 34), the position of the liquid corners of the tie triangles was eventually determined by considering that the tie lines drawn in Fig. 5 gradually changed their slope to intersect on a liquidus line passing through the different points determined by TA (Table 4).

Figure 10 shows the compounds θ, α, and δ to be in equilibrium at 727 °C with an Al-Fe-Si liquid, L. For these three solid-liquid equilibria, there is a good agreement with previously published and currently accepted equilibria (Ref 1, 2, 9, 15); the authors have simply refined the corresponding phase field boundaries. Figure 10 also shows the ternary compound γ to be in equilibrium at 727 °C with the liquid. More specifically, γ with ~20 at.% Fe and 16 to 20 at.% Si is in equilibrium with a liquid containing 3.2 to 3.5 at.% Fe

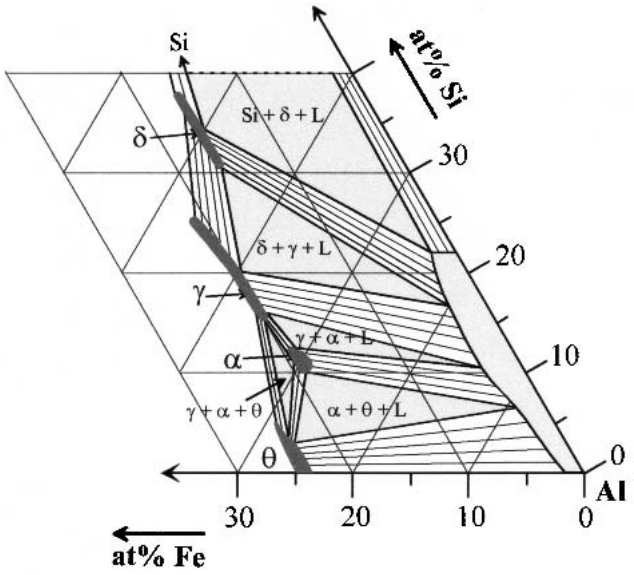

Fig. 10 Solid-liquid phase equilibria at 727 °C in the Al-Fe-Si ternary system, as experimentally refined in this work

and 10.5 to 16.5 at.% Si. Existence of that equilibrium at 727 °C can hardly be questioned; indeed, it follows from seven distinct isothermal diffusion experiments and it is corroborated by XRD characterization of crystals grown from the liquid upon cooling. Agreement with previous reports, however, is not as good as the agreement for θ, α, and δ. Rivlin et al. (Ref 2) and Ghosh (Ref 9) have reported no phase other than θ, α, δ, and Si can be in equilibrium with the liquid at 727 °C. Mondolfo (Ref 1) indicates coexistence of γ with α or δ and a liquid is possible but only at temperatures higher than 770 °C; below that value, it is the compound β instead of γ, which would be in equilibrium with the liquid. In fact, only the Al-Fe-Si diagram calculated by Liu and Chang (Ref 16) shows γ in equilibrium with the liquid near 730 °C.

5. Conclusion

The aim of the present work was to acquire more precise data on the liquid-solid phase equilibria in the Al-Fe-Si system at 727 °C and under atmospheric pressure (101,350 Pa). To achieve this goal, isothermal diffusion experiments as well as chemical and thermal analyses were performed on Al-Fe-Si mixtures with different compositions. By combining the results of the three experimental approaches, a refined isothermal section of the aluminum-rich corner of the Al-Fe-Si phase diagram has been established (Fig. 10). These refined data should be useful for a better control of materials production processes such as casting of nearly eutectic Al-Si alloys or joining steel to aluminum with Al-Si brazes.

As a major result of the present experimental investigation, it is pointed out that the ternary compound γAl_3FeSi is in equilibrium at 727 °C with an aluminum-rich Al-Fe-Si ternary liquid, L. Existence of such γ-L equilibrium at 727 °C implies occurrence upon cooling of invariant transfor-

mations about which little is presently known. Determination of the nature and temperature of these transformations will be the subject of a forthcoming paper.

References

1. L.F. Mondolfo, *Aluminium and Alloys, Structure and Properties,* Butterworth, 1976, p 282-289 (Al-Fe binary) and p 534-537 (Al-Fe-Si ternary)
2. V.G. Rivlin and G.V. Raynor, Critical Evaluation of Constitution of Al-Fe-Si System, *Int. Met. Rev.,* Vol 3, 1981, p 133-152
3. V. Stefaniay, A. Griger, and T. Turmezey, Intermetallic Phases in the Aluminium-Side Corner of AlFeSi-Alloy System, *J. Mater. Sci.,* Vol 22, 1987, p 539-546
4. H. Tanihata, T. Sugawara, K. Matsuda, and S. Ikeno, Effect of Casting Conditions on the Formation of Al-Fe-Si Intermetallic Compounds, *J. Mater. Sci.,* Vol 34, 1999, p 1205-1210
5. P. Skjerpe, Intermetallic Phases Formed During DC-Casting of an Al-0.25 wt.% Fe-0.13 wt.% Si Alloy, *Metall. Trans. A,* Vol 18A, 1987, p 189-200
6. S.G. Shabestari and J.E. Gruzleski, The Effect of Solidification Condition and Chemistry on the Formation and Morphology of Complex Intermetallic Compounds in Al-Si Alloys, *Cast Met.,* Vol 6, 1994, p 217-224
7. V. Raghavan, Al-Fe-Si, *J. Phase Equilibria,* Vol 15, Issue 4 1994, p 414-416
8. M.H. Mulazimoglu, A. Zaluska, J.E. Gruzleski, and F. Paray, Electron Microscope Study of Al-Fe-Si Intermetallics in 6201 Aluminum Alloy, *Metall. Mater. Trans. A,* Vol 27A, 1996, p 929-936
9. G. Ghosh, Al-Fe-Si, *Ternary Alloys,* G. Petzow and G. Effenberg, Ed., Vol 5, VCH, Weinheim, Germany, 1992, p 394-438
10. G.V. Raynor and V.G. Rivlin, *Phase Equilibria in Iron Ternary Alloys,* The Institute of Metals, 1988, p 122-139
11. M. Vybornov, P. Rogl, and F. Sommer, On the Thermodynamic Stability and Solid Solution Behavior of the Phases τ_5-$Fe_2Al_{7.4}Si$ and τ_6-$Fe_2Al_9Si_2$, *J. Alloys Compd.,* Vol 247, 1997, p 154-157
12. Y. Li, P. Ochin, A. Quivy, P. Telolahy, and B. Legendre, Enthalpy of Formation of Al-Fe-Si Alloys (τ_5, τ_{10}, τ_1, τ_9), *J. Alloys Compd.,* Vol 298, 2000, p 198-202
13. Y. Li and B. Legendre, Enthalpy of Formation of Al-Fe-Si Alloys II (τ_6, τ_2, τ_3, τ_8, τ_4), *J. Alloys Compd.,* Vol 302, 2000, p 187-191
14. J.C. Anglezio, C. Servant, and I. Ansara, Contribution to the Experimental and Thermodynamic Assessment of the Al-Ca-Fe-Si System—I. Al-Ca-Fe, Al-Ca-Si, Al-Fe-Si and Ca-Fe-Si Systems, *CALPHAD,* Vol 18, 1994, p 273-309
15. P. Gilgien, "Calcul de cartes de microstructures de solidification pour le système Al-Fe-Si," (Calculation of Microstructure Solidification Maps for the Al-Fe-Si System), Doctorat thesis, EPFL Lausanne, Switzerland, 1996
16. Z.K. Liu and Y.A. Chang, Thermodynamic Assessment of the Al-Fe-Si System, *Metall. Mater. Trans. A,* Vol 30A, 1999, p 1081-1095
17. V. Raghavan, Al-Fe-Si, *J. Phase Equilibria,* Vol 23, 2002, p 362-366
18. A. Lendvai, Phase Diagram of the Al-Fe System up to 45 Mass% Iron, *J. Mater. Sci.,* Vol 5, 1986, p 1219-1220
19. A. Griger, V. Stefaniay, and T. Turmezey, Crystallographic Data and Chemical Compositions of Al-Rich Al-Fe Intermetallic Phases, *Z. Metallkde.,* Vol 77, 1986, p 30-35
20. S. Pontevichi, "Réactivité chimique dans le système Al-Fe-Si," (Chemical Reactions at the Interface between Solid Iron and Liquid Al-Si Alloys), Doctorat thesis, UCBL1, Lyon, France, 2004
21. J. Grin, U. Burkhardt, M. Ellner, and K. Peters, Refinement of the Fe_4Al_{13} Structure and its Relationship to the Quasihomological Homeotypical Structures, *Z. Kristallogr.,* Vol 209, 1994, p 479-487
22. R. Hultgren, P.D. Desai, D.T. Hawkins, M. Gleiser, K.K. Kelley, and D.T. Wagman, *Selected Values of the Thermodynamic Properties of Binary Alloys,* ASM International, 1973
23. A. Griger, Powder Diffraction Data for the αH Intermetallic Phases with Slight Variation in Composition in the System Al-Fe-Si, *Powder Diffraction,* Vol 2, 1987, p 31-35
24. T. Turmezey, V. Stefaniay, and A. Griger, AlFeSi Phases in Al, *Key Eng. Mater.,* Vol 44-45, 1990, p 57-58
25. D. Munson, A Clarification of the Phases Occurring in Al-Rich Al-Fe-Si Alloys, with Particular Reference to the Ternary Phase α-AlFeSi, *J. Inst. Met.,* Vol 95, 1967, p 217-219
26. R.N. Corby and P.J. Black, The Structure of α-(AlFeSi) by Anomalous-Dispersion Methods, *Acta Crystallogr.,* Sec. B33, 1977, p 3468-3475
27. A.M. Zakharov, I.T. Guldin, A.A. Arnold, and Yu.A. Matsenko, Al-Si-Fe within the Concentration Ranges of 10-14 %Si and 0-3 %Fe, *Izv. Akad. Nauk SSSR Metal.,* Vol 3, 1988, p 178-181
28. C. Romming, V. Hansen, and J. Gjonnes, Crystal Structure of β-$Al_{4.5}FeSi$, *Acta Crystallogr.,* Sec. B50, 1994, p 307-312
29. C. Gueneau, C. Servant, F. d'Yvoire, and N. Rodier, $FeAl_3Si_2$, *Acta Crystallogr.,* Sec. C51, 1995, p 177-179
30. N.V. German, V.E. Zavodnik, T.I. Yanson, and O.S. Zarechnyuk, Crystal Structure of $FeAl_2Si$, *Kristallographiya,* Vol 34, 1989, p 738-739
31. N.V. German, V.K. Bel'skii, T.I. Yanson, and O.S. Zarechnyuk, Crystal Structure of the Compound $Fe_{1.7}Al_4Si$, *Kristallographia,* Vol 34, 1989, p 735-737
32. M. Hansen, *Constitution of Binary Alloys,* McGraw-Hill, 1958, p 91
33. T.B. Massalski, *Binary Alloy Phase Diagrams,* ASM International, 1986, p 111-112
34. A. Prince, *Alloy Phase Equilibria,* Elsevier, Amsterdam, 1966